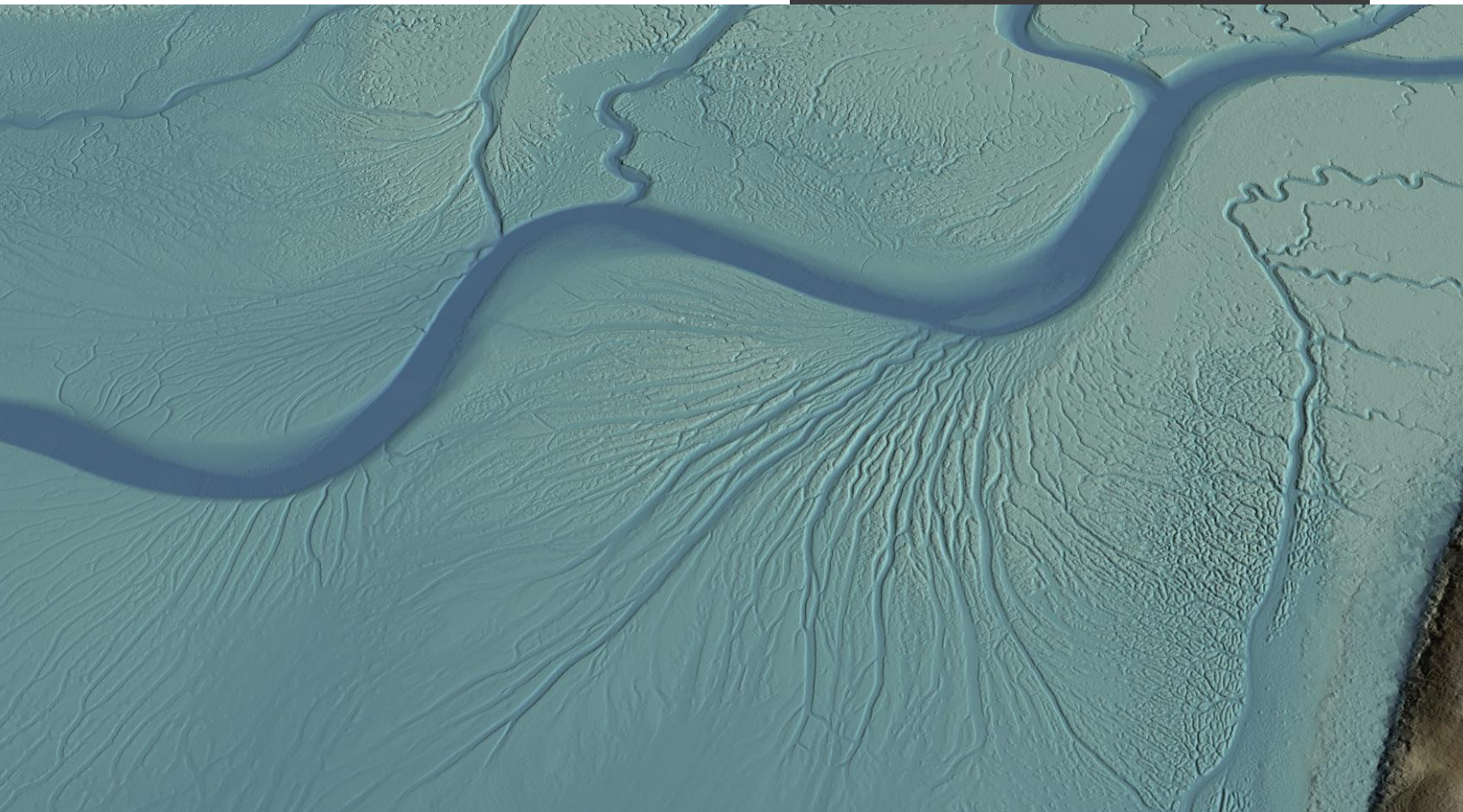


September 9, 2022
Revised: October 3, 2022



Morro Bay, California

Topobathymetric Lidar Technical Data Report

Prepared For:



Morro Bay National Estuary Program

Attn: Ann Kitajima
601 Embarcadero, Suite 11
Morro Bay, CA 93442

Prepared By:



NV5 Geospatial Corvallis
1100 NE Circle Blvd, Ste. 126
Corvallis, OR 97330
PH: 541-752-1204

TABLE OF CONTENTS

INTRODUCTION.....	1
Deliverable Products.....	2
ACQUISITION.....	4
Planning.....	4
Environmental Conditions: Turbidity and Secchi Depth Readings.....	5
Airborne Lidar Survey.....	8
Ground Survey.....	10
Base Station.....	10
Ground Survey Points (GSPs).....	11
PROCESSING.....	13
Topobathymetric Lidar Data.....	13
Bathymetric Refraction.....	16
Topobathymetric DEMs.....	16
RESULTS & DISCUSSION.....	17
Bathymetric Lidar.....	17
Mapped Bathymetry Coverage.....	17
Lidar Point Density.....	18
First Return Point Density.....	18
Bathymetric and Ground Classified Point Densities.....	18
Lidar Accuracy Assessments.....	21
Lidar Non-Vegetated Vertical Accuracy.....	21
Lidar Bathymetric Vertical Accuracies.....	24
Lidar Relative Vertical Accuracy.....	26
Lidar Horizontal Accuracy.....	27
CERTIFICATIONS.....	28
SELECTED IMAGES.....	29
GLOSSARY.....	31
APPENDIX A - ACCURACY CONTROLS.....	32

Cover Photo: An image of the topobathymetric bare earth model looking over Morro Bay. The model was generated using the ground and bathymetric bottom lidar classifications and colored by elevation.

LIST OF FIGURES

Figure 1: Location map of the Morro Bay site in California.....	3
Figure 2: Tide Predictions at 9412110, Port San Luis CA during the time of lidar acquisition	6
Figure 3: These photos, taken by NV5's ground survey team, display water clarity conditions and eel grass within Morro Bay on June 14, 2022, near the time of lidar acquisition.	7
Figure 4: Flightline map of Morro Bay, California project.....	9
Figure 5: Ground survey location map.....	12
Figure 6: Frequency distribution of first return densities per 100 x 100 m cell	19
Figure 7: Frequency distribution of ground and bathymetric bottom classified return densities per 100 x 100 m cell	19
Figure 8: First return and ground and bathymetric bottom density map for the Morro Bay site (100 m x 100 m cells).....	20
Figure 9: Frequency histogram for unclassified LAS deviation from ground check point values.....	22
Figure 10: Frequency histogram for lidar bare earth DEM deviation from ground check point values.....	23
Figure 11: Frequency histogram for lidar surface deviation ground control point values	23
Figure 12: Frequency histogram for lidar surface deviation from submerged check point values	24
Figure 13: Frequency histogram for lidar surface deviation from wetted edge check point values	25
Figure 14: Frequency plot for relative vertical accuracy between flight lines	26
Figure 15: A top down view of the Morro Bay area of interest. This image was created from the lidar bare earth elevation model colored by elevation.....	29
Figure 16: A top down view of the Morro Bay area of interest. This image was created from the lidar bare earth elevation model colored by elevation.....	30

LIST OF TABLES

Table 1: Acquisition dates, acreage, and data types collected on the Morro Bay site.....	2
Table 2: Deliverable product coordinate reference system information	2
Table 3: Lidar products delivered for the Morro Bay site	2
Table 4: Water Clarity Observations for lidar flights	5
Table 5: Lidar specifications and survey settings	8
Table 6: Monument positions for the Morro Bay acquisition. Coordinates are on the NAD83 (2011) datum, epoch 2010.00	10
Table 7: NV5 ground survey equipment identification.....	11
Table 8: ASPRS LAS classification standards applied to the Morro Bay dataset.....	14
Table 9: Lidar processing workflow	15
Table 10: Average lidar point densities.....	18
Table 11: Absolute accuracy results	22
Table 12: Bathymetric Vertical Accuracy for the Morro Bay Project	24
Table 13: Relative accuracy results	26
Table 14: Horizontal Accuracy	27

INTRODUCTION

This image shows a scenic view of sailboats and an otter in the Morro Bay AOI. Otters are helping to revitalize the eelgrass population by removing grazers.



In June 2022, NV5 was contracted by the National Oceanic and Atmospheric Administration Office of Coastal Management Office of Coastal Management (NOAA) and Morro Bay National Estuary Program (NEP) to collect topobathymetric light detection and ranging (lidar) data in the summer of 2022 for the Morro Bay site in San Luis Obispo County, California. This project was completed in partnership between NOAA Office of Coastal Management and the NEP. The Morro Bay area of interest (AOI) covers approximately 3,593 acres over Morro Bay, including the Morro Bay Estuary and roughly 3.6 miles of coastline (Figure 1). Traditional near-infrared (NIR) lidar was fully integrated with green wavelength return data (bathymetric) lidar to provide a seamless topobathymetric lidar dataset.

Data was collected to aid NOAA in assessing the channel morphology and topobathymetric surface of the study area to support and inform coastal resource and watershed managers on decisions relating to the “Building Climate Resilience and Improving Water Quality through Eelgrass Restoration in Morro Bay” project. This project monitors eelgrass, which declined between 2007 and 2011. The decline of eelgrass led to increased sediment erosion and, therefore, an effort to replant more eelgrass. Many organisms such as otters are reliant on the eelgrass for either food or shelter. Otters play a key role in restoration efforts by removing grazers. The lidar data will assist in quantifying change in eelgrass distribution over time as well as sediment transport and sea level rise.

This report accompanies the delivered integrated topobathymetric lidar and documents contract specifications, data acquisition procedures, processing methods, and analysis of the final dataset including lidar accuracy, maximum depth penetration, and density. Acquisition dates and acreage are shown in Table 1, a complete list of contracted deliverables provided to NOAA is shown in Table 2 and Table 3, and the project extent is shown in Figure 1.

Table 1: Acquisition dates, acreage, and data types collected on the Morro Bay site

Project Site	Contracted Acres	Acquisition Dates	Data Type
Morro Bay, California	3,593	6/14/2022	High Resolution Topobathymetric Lidar

Deliverable Products

Table 2: Deliverable product coordinate reference system information

Projection	Horizontal Datum	Vertical Datum	Units
UTM Zone 10 North	NAD83(2011)	NAVD88(GEOID12B)	Meters

Table 3: Lidar products delivered for the Morro Bay site

Product Type	File Type	Product Details
Points	LAS v.1.4 (*.las)	<ul style="list-style-type: none"> All Classified Returns
Rasters	GeoTIFFs (*.tif)	<ul style="list-style-type: none"> 1.0 Meter Void Clipped Topobathymetric Bare Earth Digital Elevation Model (DEM)
Vectors	Shapefiles (*.shp)	<ul style="list-style-type: none"> Project Boundary Lidar and DEM Tile Index Bathymetric Coverage Shape
Vectors	ESRI File Geodatabase (*.gdb)	<ul style="list-style-type: none"> Ground Survey Points and Monument Locations Flightline Index Water's Edge Breaklines
Reports	Extensible Markup Language (*.xml)	<ul style="list-style-type: none"> Metadata
Reports	Adobe Acrobat (*.pdf)	<ul style="list-style-type: none"> Lidar Technical Data Report



Figure 1: Location map of the Morro Bay site in California.

NV5's ground acquisition equipment set up in the Morro Bay lidar study area.



Planning

In preparation for lidar data collection, NV5 reviewed the project area and developed a specialized flight plan to ensure complete coverage of the Morro Bay lidar study area at the target combined point density of ≥ 8 points/m². Acquisition parameters including orientation relative to terrain, flight altitude, pulse rate, scan angle, and ground speed were adapted to optimize flight paths and flight times, while meeting all contract specifications.

Factors such as satellite constellation availability and weather windows must be considered during the planning stage. Any weather hazards or conditions affecting the flight were continuously monitored due to their potential impact on the daily success of airborne and ground operations. Logistical considerations including private property access and potential air space restrictions were reviewed. Flight times were chosen for optimal tide conditions (Table 4, Figure 2). Acquisition took place during low tide to map more of the landscape. However, an additional mission was flown at high tide along the beach in an effort to capture this area under better surf zone water clarity conditions. Therefore, this project encompasses 2 tidal windows, a low and high tide. In addition, water clarity (Figure 3) and turbidity (Table 4) were measured around the time of acquisition.

Environmental Conditions: Turbidity and Secchi Depth Readings

In order to assess water clarity conditions prior to and during lidar collection, NV5 collected turbidity measurements, secchi depth readings, and wind speed and direction measurements. Readings were collected at three locations throughout the project site on June 14, 2022. Turbidity observations were recorded three times to confirm measurements. Table 4 below provides turbidity and secchi depth results per site on each day of data collection as applicable. High turbidity, like that in Table 4, can account for a lower bathymetric coverage.

Table 4: Water Clarity Observations for lidar flights

Date	Time (UTC-7h)	Location	Latitude	Longitude	Turbidity Read 1 (NTU)	Turbidity Read 2 (NTU)	Turbidity Read 3 (NTU)	Secchi Depth (m)	Wind Speed (mph)
6/14/22	10:00	Boat rental dock at Morro Bay State Park	35° 21' 56.322"	-120° 51' 13.183"	25.3	25.4	25.5	1.20	5 S
6/14/22	10:30	Public dock at Tidelands Park	35° 21' 34.2396"	-120° 51' 6.772"	23.0	23.0	22.3	1.77	5 S
6/14/22	11:00	Public dock at intersection of Embarcadero and Front Street	35° 20' 45.366"	-120° 50' 36.146"	22.3	22.1	22.3	1.95	5 SW

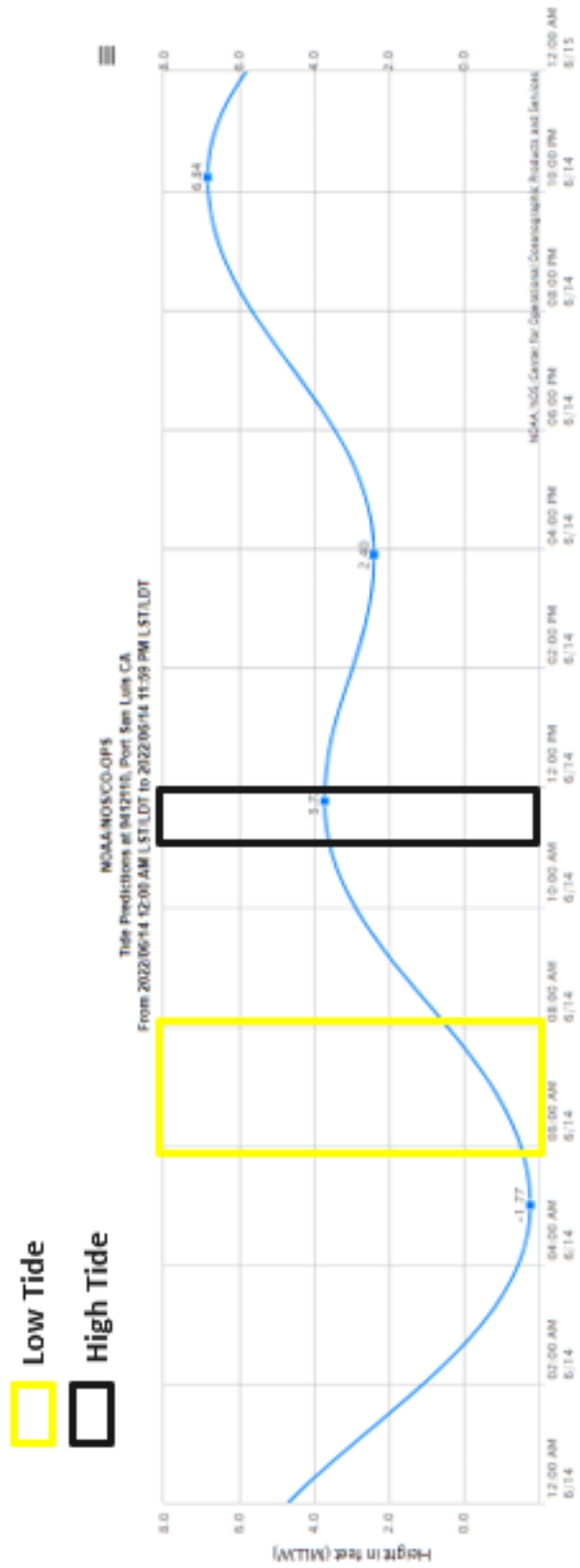


Figure 2: Tide Predictions at 9412110, Port San Luis CA during the time of lidar acquisition



Figure 3: These photos, taken by NV5's ground survey team, display water clarity conditions and eel grass within Morro Bay on June 14, 2022, near the time of lidar acquisition.

Airborne Lidar Survey

The lidar survey was accomplished using a Riegl VQ-880-G-II green laser system mounted in a Cessna Caravan. The Riegl VQ-880-G-II boasts a high repetition pulse rate (up to 550 kHz), high scanning speed, small laser footprint, wide field of view, and integrated green and NIR wavelength lasers which allows for seamless collection of high-resolution topographic and bathymetric surface data. The green wavelength ($\lambda=532$ nm) laser is capable of collecting high resolution topography data, as well as penetrating the water surface with minimal spectral absorption by water. The integrated NIR laser ($\lambda=1064$ nm) adds additional topography data and aids in water surface modeling. The recorded waveform enables range measurements for all discernible targets for a given pulse. The Riegl VQ-880II laser system can record unlimited range measurements (returns) per pulse, however a maximum of 15 returns can be stored due to LAS v1.4 file limitations. It is not uncommon for some types of surfaces (e.g., dense vegetation or water) to return fewer pulses to the lidar sensor than the laser originally emitted. The discrepancy between first return and overall delivered density will vary depending on terrain, land cover, and the prevalence of water bodies. All discernible laser returns were processed for the output dataset. Table 5 summarizes the settings used to yield an average pulse density of ≥ 8 pulses/m² over the Morro Bay project area.

Table 5: Lidar specifications and survey settings

Parameter	Green Laser	NIR Laser
Acquisition Dates	6/14/2022	6/14/2022
Aircraft Used	Cessna Caravan	Cessna Caravan
Sensor	Riegl	Riegl
Laser	VQ-880-GII-Green	VQ-880GII-IR
Maximum Returns	14	13
Resolution/Density	Average 8 pulses/m ²	Average 8 pulses/m ²
Nominal Pulse Spacing	0.35 m	0.35 m
Survey Altitude (AGL)	400 m	400 m
Survey speed	120 knots	120 knots
Field of View	40°	42°
Mirror Scan Rate	80 Lines per Second	Uniform Point Spacing
Target Pulse Rate	200 kHz	300 kHz
Pulse Length	1.5 ns	3 ns
Laser Pulse Footprint Diameter	28 cm	8 cm
Central Wavelength	532 nm	1064 nm
Pulse Mode	Multiple Times Around (MTA)	Multiple Times Around (MTA)
Beam Divergence	0.7 mrad	0.2 mrad
Swath Width	291 m	307 m
Swath Overlap	30%	30%
Intensity	16-bit	16-bit
Vertical Accuracy	RMSE _z ≤ 6 cm	RMSE _z ≤ 6 cm
Horizontal Accuracy	Horizontal Accuracy ≤ 4 feet	Horizontal Accuracy ≤ 4 feet

To accurately solve for laser point position (geographic coordinates x, y and z), the positional coordinates of the airborne sensor and the attitude of the aircraft were recorded continuously throughout the lidar data collection mission. Position of the aircraft was measured twice per second (2 Hz) by an onboard differential GPS unit, and aircraft attitude was measured 200 times per second (200 Hz) as pitch, roll and yaw (heading) from an onboard inertial measurement unit (IMU). To allow for post-processing correction and calibration, aircraft and sensor position and attitude data are indexed by GPS time.



Figure 4: Flightline map of Morro Bay, California project.

Ground Survey

Ground control surveys, including monumentation, and ground survey points (GSPs), were conducted to support the airborne acquisition. Ground control data were used to geospatially correct the aircraft positional coordinate data and to perform quality assurance checks on final lidar data.

Base Station

Base station locations were selected with consideration for satellite visibility, field crew safety, and optimal location for GSP coverage. NV5 utilized one previously established monument for the Morro Bay lidar project (Table 6, Figure 5). NV5's professional land surveyor, Evon Silvia (CAPLS#9401) oversaw and certified the ground survey.



Existing NGS Monument

Table 6: Monument positions for the Morro Bay acquisition. Coordinates are on the NAD83 (2011) datum, epoch 2010.00

Monument ID	Latitude	Longitude	Ellipsoid (meters)
MB_9R	35° 22' 19.76539" N	120° 51' 34.76616" W	-29.859

NV5 utilized static Global Navigation Satellite System (GNSS) data collected at 1 Hz recording frequency for each base station. During post-processing, the static GNSS data were triangulated with nearby Continuously Operating Reference Stations (CORS) using the Online Positioning User Service (OPUS¹) for precise positioning. Multiple independent sessions over the same monument were processed to confirm antenna height measurements and to refine position accuracy.

¹ OPUS is a free service provided by the National Geodetic Survey to process corrected monument positions. [OPUS website](#)

Ground Survey Points (GSPs)

Ground survey points were collected using real time kinematic (RTK) survey techniques. For RTK surveys, a roving receiver receives corrections from a nearby base station or Real-Time Network (RTN) via radio or cellular network, enabling rapid collection of points with relative errors less than 1.5 cm horizontal and 2.0 cm vertical. RTK surveys record data while stationary for at least five seconds, calculating the position using at least three one-second epochs. All GSP measurements were made during periods with a Position Dilution of Precision (PDOP) of ≤ 3.0 with at least six satellites in view of the stationary and roving receivers. See Table 7 for NV5 ground survey equipment information.

GSPs were collected in areas where good satellite visibility was achieved on paved roads and other hard surfaces such as gravel or packed dirt roads. GSP measurements were not taken on highly reflective surfaces such as center line stripes or lane markings on roads due to the increased noise seen in the laser returns over these surfaces. GSPs were collected within as many flightlines as possible; however, the distribution of GSPs depended on ground access constraints and monument locations and may not be equably distributed throughout the study area (Figure 5).

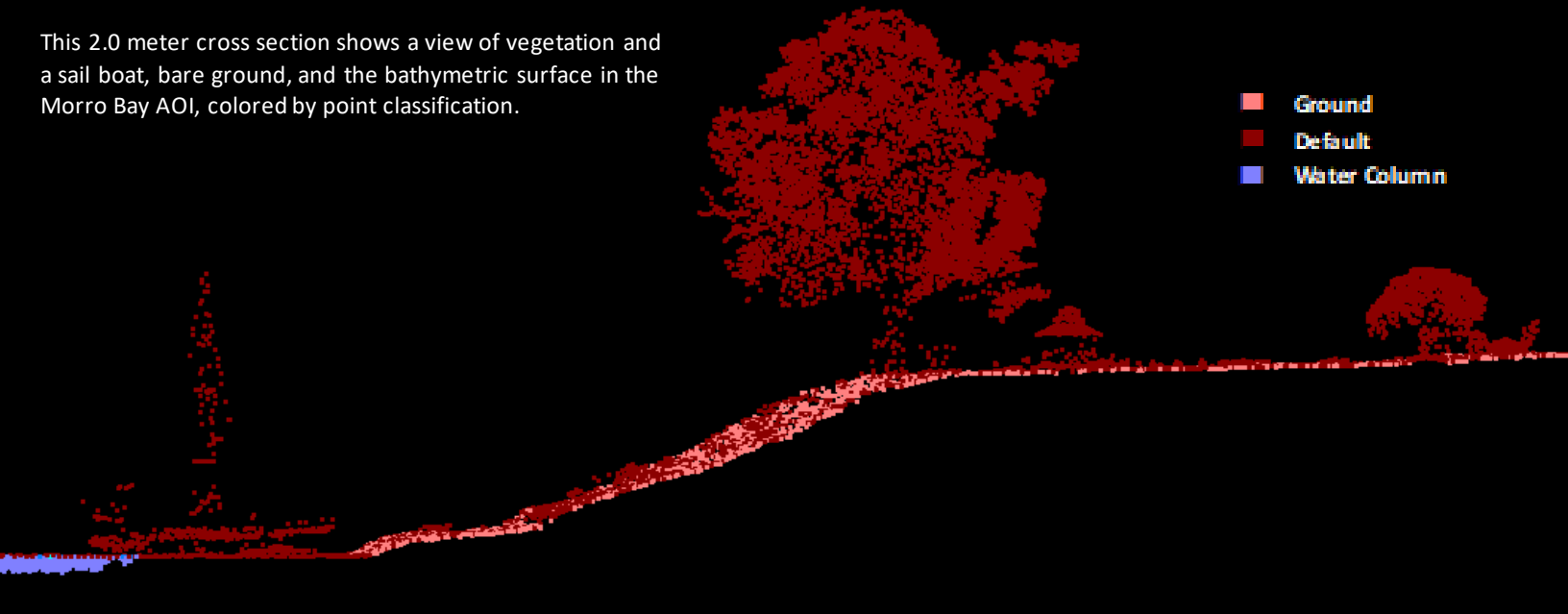
Table 7: NV5 ground survey equipment identification

Receiver Model	Antenna	OPUS Antenna ID	Use
Trimble R7	Zephyr GNSS Geodetic Model 2 RoHS	TRM57971.00	Static
Trimble R12	Integrated Antenna	TRMR12	Rover



Figure 5: Ground survey location map

This 2.0 meter cross section shows a view of vegetation and a sail boat, bare ground, and the bathymetric surface in the Morro Bay AOI, colored by point classification.



Topobathymetric Lidar Data

Upon completion of the lidar data acquisition, NV5 processing staff initiated a suite of automated and manual techniques to process the data into the requested deliverables. Processing tasks include d GPS control computations, smoothed best estimate trajectory (SBET) calculations, kinematic corrections, calculation of laser point position including refraction of green laser returns through water, sensor and data calibration for optimal relative and absolute accuracy, and lidar point classification (Table 8). A brief description of all processing tasks is shown in Table 9.

Table 8: ASPRS LAS classification standards applied to the Morro Bay dataset

Classification Number	Classification Name	Classification Description
1	Default/Unclassified	Laser returns that are not included in the ground class, composed of vegetation and anthropogenic features
2	Ground	Laser returns that are determined to be ground using automated and manual cleaning algorithms
7W	Noise/Withheld	Laser returns that are often associated with artificial points below the ground surface
9	Water	Laser returns that are determined to be water using automated and manual cleaning algorithms
18W	High Noise/Withheld	Laser returns that are often associated with birds or scattering from reflective surfaces
40	Bathymetric Bottom	Refracted green laser returns that fall within the water's edge breakline which characterize the submerged topography.
41	Water Surface	Green laser returns that are determined to be water surface points using automated and manual cleaning algorithms.
45	Water Column	Refracted Riegl sensor returns that are determined to be water using automated and manual cleaning algorithms.

Table 9: Lidar processing workflow

Lidar Processing Step	Software Used
<p>Resolve kinematic corrections for aircraft position data using kinematic aircraft GPS and static ground GPS data. Develop a smoothed best estimate of trajectory (SBET) file that blends post-processed aircraft position with sensor head position and attitude recorded throughout the survey.</p>	<p>POSPac MMS v.8.7</p>
<p>Calculate laser point position by associating SBET position to each laser point return time, scan angle, intensity, etc. Create raw laser point cloud data for the entire survey in *.las (ASPRS v. 1.4) format. Convert data to orthometric elevations by applying a geoid correction.</p>	<p>RiUnite v1.0.1</p>
<p>Using ground classified points per each flight line, test the relative accuracy. Perform automated line-to-line calibrations for system attitude parameters (pitch, roll, heading), mirror flex (scale) and GPS/IMU drift. Calculate calibrations on ground classified points from paired flight lines and apply results to all points in a flight line. Use every flight line for relative accuracy calibration.</p>	<p>BayesMap-StripAlign v.2.19</p>
<p>Apply refraction correction to all subsurface returns.</p>	<p>Las Monkey 2.6.6 (NV5 proprietary software)</p>
<p>Classify resulting data to ground and other client designated ASPRS classifications. Assess statistical absolute accuracy via direct comparisons of ground classified points to ground control survey data.</p>	<p>TerraScan v.19 TerraModeler v.19</p>
<p>Generate bare earth models as triangulated surfaces. Clip bare earth DEMs to remove bathymetric void areas. Export all surface models in GeoTIFFs at a 1.0 meter pixel resolution.</p>	<p>Las Product Creator 3.0 (NV5 proprietary software) ArcMap v. 10.8.1</p>

Bathymetric Refraction

Green lidar pulses that enter the water column must have their position corrected for refraction of the light beam as it passes through the water and its resulting decreased speed. NV5 has developed proprietary software (Las Monkey) to perform this processing based on Snell's law. The first step is to develop a water surface model (WSM) from the NIR lidar water surface returns. The water surface model used for refraction is generated using NIR points within the breaklines defining the water's edge. Points are filtered and edited to obtain the most accurate representation of the water surface and are used to create a water surface model TIN. A TIN model is preferable to a raster based water surface model to obtain the most accurate angle of incidence during refraction.

Once the WSM is generated, the Las Monkey refraction software then intersects the partially submerged green pulses with the WSM to determine the angle of incidence with the water surface and the submerged component of the pulse vector. This provides the information necessary to correct the position of underwater points by adjusting the submerged vector length and orientation. After refraction, the points are compared against bathymetric check points to assess accuracy.

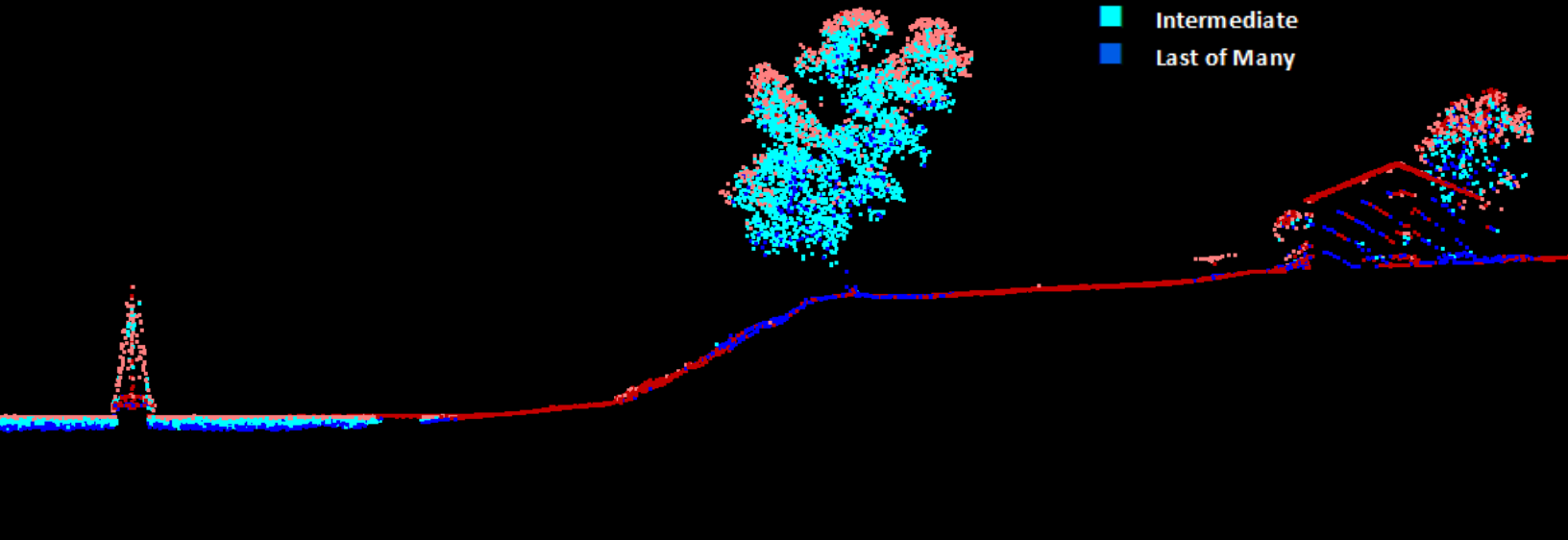
Topobathymetric DEMs

Bathymetric bottom returns from lidar can be limited by depth, water clarity, and bottom surface reflectivity. Water clarity and turbidity affects the depth penetration capability of the green wavelength laser with returning laser energy diminishing by scattering throughout the water column. Additionally, the bottom surface must be reflective enough to return remaining laser energy back to the sensor at a detectable level. Although the predicted depth penetration range of the Riegl VQ-880-G sensor is 1.5 Secchi depths on brightly reflective surfaces, it is not unexpected to have bathymetric bottom returns in turbid or non-reflective areas.

As a result, creating digital elevation models (DEMs) presents a challenge with respect to interpolation of areas with no returns. Traditional DEMs are "unclipped", meaning areas lacking ground returns are interpolated from neighboring ground returns (or breaklines in the case of hydro-flattening), with the assumption that the interpolation is close to reality. In bathymetric modeling, these assumptions are prone to error because a lack of bathymetric returns can indicate a change in elevation that the laser can no longer map due to increased depths. The resulting void areas may suggest greater depths, rather than similar elevations from neighboring bathymetric bottom returns. Therefore, NV5 created a water polygon with bathymetric coverage to delineate areas with successfully mapped bathymetry. This shapefile was used to control the extent of the delivered clipped topobathymetric model to avoid false triangulation (interpolation from TIN'ing) across areas in the water with no bathymetric returns.

This 2.0 meter cross section shows a view of an oceanside park and a sailboat in the Morro Bay site, colored by echo.

- Only Echo
- First of Many
- Intermediate
- Last of Many



Bathymetric Lidar

In order to determine the capability and effectiveness of the bathymetric lidar, several parameters were considered such as the maximum depth penetration below the water surface, bathymetric return density, and spatial accuracy.

Mapped Bathymetry Coverage

Some areas within the project area prevented lidar penetration to the bathymetric bottom due to environmental factors including dense vegetation, near shore surf/whitewater, and turbidity. A bathymetric coverage polygon shapefile was created to delineate areas where bathymetry was successfully mapped.

This shapefile was used to control the extent of the delivered clipped topo-bathymetric model and to avoid false triangulation across areas in the water with no returns. Insufficiently mapped areas were identified by triangulating bathymetric bottom points with an edge length maximum of 4.56 meters. This ensured all areas of no returns ($> 9 \text{ m}^2$) were identified as data voids. Overall NV5 Geospatial successfully mapped 31.32% of the bathymetric area in the Morro Bay AOI. This is lower than the percent coverage in the 2019 lidar collect likely because of higher turbidity conditions and lack of sonar integration. The maximum recorded depth for the Morro Bay topobathymetric dataset was 7.33 meters.

Lidar Point Density

First Return Point Density

The acquisition parameters were designed to acquire an average first-return density of 8 points/m². First return density describes the density of pulses emitted from the laser that return at least one echo to the system. Multiple returns from a single pulse were not considered in first return density analysis. Some types of surfaces (e.g., breaks in terrain, water, and steep slopes) may have returned fewer pulses than originally emitted by the laser.

First returns typically reflect off the highest feature on the landscape within the footprint of the pulse. In forested or urban areas the highest feature could be a tree, building or power line, while in areas of unobstructed ground, the first return will be the only echo and represents the bare earth surface.

The average first-return density of the Morro Bay lidar project was 29.45 points/m² (Table 10). The statistical and spatial distributions of all first return densities per 100 m x 100 m cell are portrayed in Figure 6 and Figure 8.

Bathymetric and Ground Classified Point Densities

The density of ground classified lidar returns and bathymetric bottom returns were also analyzed for this project. Terrain character, land cover, and ground surface reflectivity all influenced the density of ground surface returns. In vegetated areas, fewer pulses may have penetrated the canopy, resulting in lower ground density. Similarly, the density of bathymetric bottom returns was influenced by turbidity, depth, and bottom surface reflectivity. In turbid areas, fewer pulses may have penetrated the water surface, resulting in lower bathymetric density.

The ground and bathymetric bottom classified density of lidar data for the Morro Bay project was 11.70 points/m² (Table 10). The statistical and spatial distributions ground classified and bathymetric bottom return densities per 100 m x 100 m cell are portrayed in Figure 7 and Figure 8.

Additionally, for the Morro Bay project, density values of only lidar bathymetric bottom returns were calculated for areas containing at least one lidar bathymetric bottom return. Areas lacking lidar bathymetric returns were not considered in calculating an average density value. Within the successfully mapped area, a bathymetric bottom return density of 3.49 points/m² was achieved.

Table 10: Average lidar point densities

Density Type	Point Density
First Returns	29.45 points/m ²
Ground and Bathymetric Bottom Classified Returns	11.70 points/m ²
Lidar Bathymetric Bottom Classified Returns	3.49 points/m ²

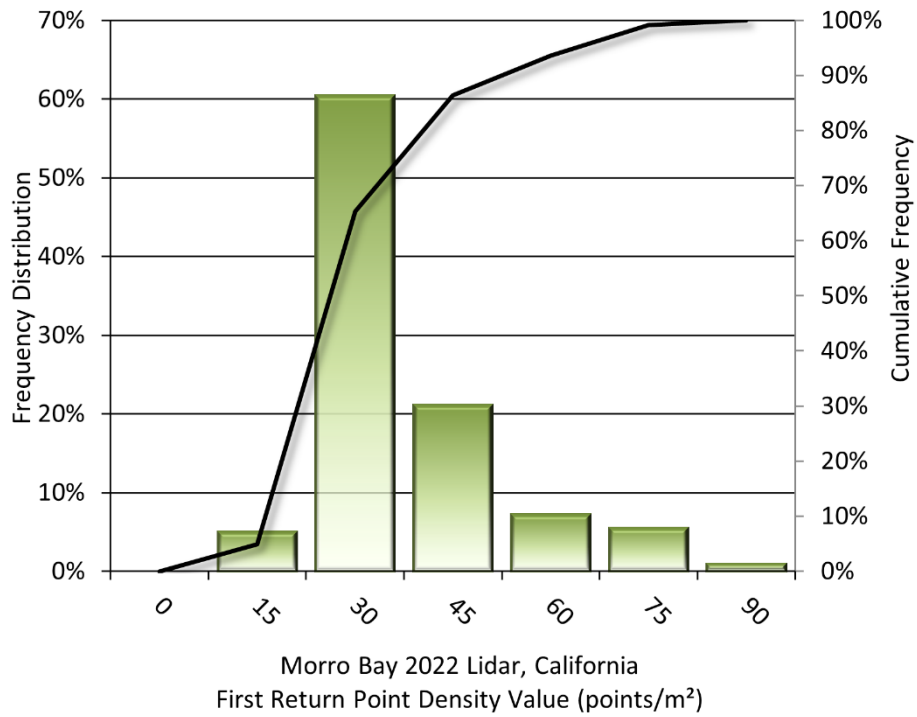


Figure 6: Frequency distribution of first return densities per 100 x 100 m cell

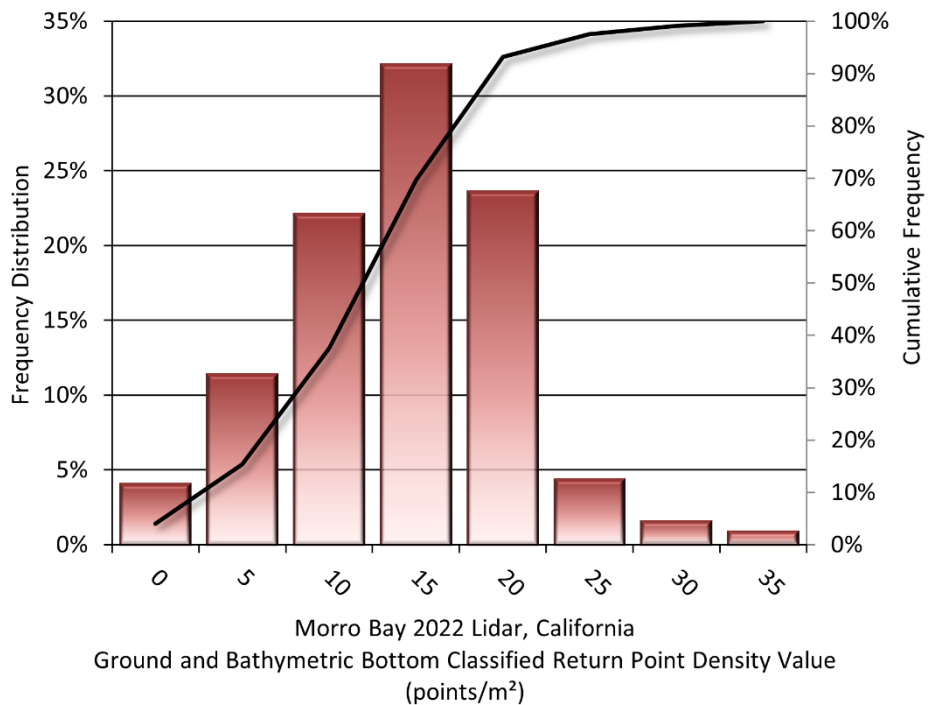


Figure 7: Frequency distribution of ground and bathymetric bottom classified return densities per 100 x 100 m cell

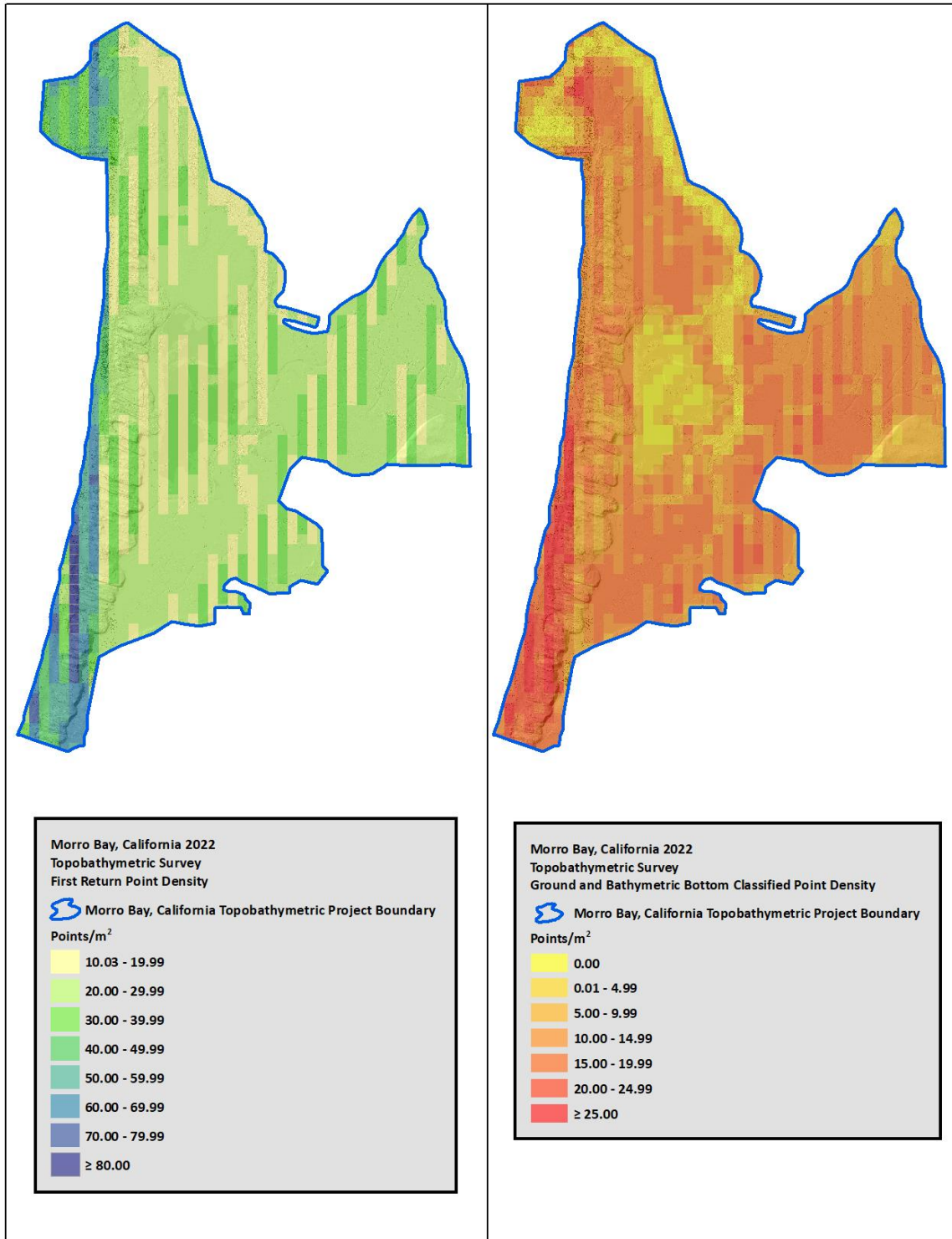


Figure 8: First return and ground and bathymetric bottom density map for the Morro Bay site (100 m x 100 m cells)

Lidar Accuracy Assessments

The accuracy of the lidar data collection can be described in terms of absolute accuracy (the consistency of the data with external data sources) and relative accuracy (the consistency of the dataset with itself). See Appendix A for further information on sources of error and operational measures used to improve relative accuracy.

Lidar Non-Vegetated Vertical Accuracy

Absolute accuracy was assessed using Non-vegetated Vertical Accuracy (NVA) reporting designed to meet guidelines presented in the FGDC National Standard for Spatial Data Accuracy². NVA compares known ground check point data that were withheld from the calibration and post-processing of the lidar point cloud to the triangulated surface generated by the unclassified lidar point cloud as well as the derived gridded bare earth DEM. NVA is a measure of the accuracy of lidar point data in open areas where the lidar system has a high probability of measuring the ground surface and is evaluated at the 95% confidence interval ($1.96 * RMSE$), as shown in Table 11.

The mean and standard deviation (σ) of divergence of the ground surface model from ground check point coordinates are also considered during accuracy assessment. These statistics assume the error for x, y and z is normally distributed, and therefore the skew and kurtosis of distributions are also considered when evaluating error statistics. For the Morro Bay survey, 21 NVA check points were withheld from the calibration and post-processing of the lidar point cloud, with resulting non-vegetated vertical accuracy of 0.049 meters as compared to the unclassified LAS, and 0.052 meters against the bare earth DEM, with 95% confidence (Figure 9 and Figure 10).

NV5 also assessed absolute accuracy using 91 ground control points. Although these points were used in the calibration and post-processing of the lidar point cloud, they still provide a good indication of the overall accuracy of the lidar dataset, and therefore have been provided in Table 11 and Figure 11.

² Federal Geographic Data Committee, ASPRS POSITIONAL ACCURACY STANDARDS FOR DIGITAL GEOSPATIAL DATA EDITION 1, Version 1.0, NOVEMBER 2014. [ASPRS-POSITIONAL-ACCURACY-STANDARDS-FOR-DIGITAL-GEOSPATIAL-DATA website](#)

Table 11: Absolute accuracy results

Parameter	NVA, as compared to Unclassified LAS	NVA, as compared to Bare Earth DEM	Ground Control Points
Sample	21 points	21 points	91 points
95% Confidence (1.96*RMSE)	0.049 m	0.052 m	0.043 m
Average	0.010 m	0.009 m	-0.002 m
Median	0.008 m	0.013 m	-0.002 m
RMSE	0.025 m	0.026 m	0.022 m
Standard Deviation (1σ)	0.023 m	0.025 m	0.022 m

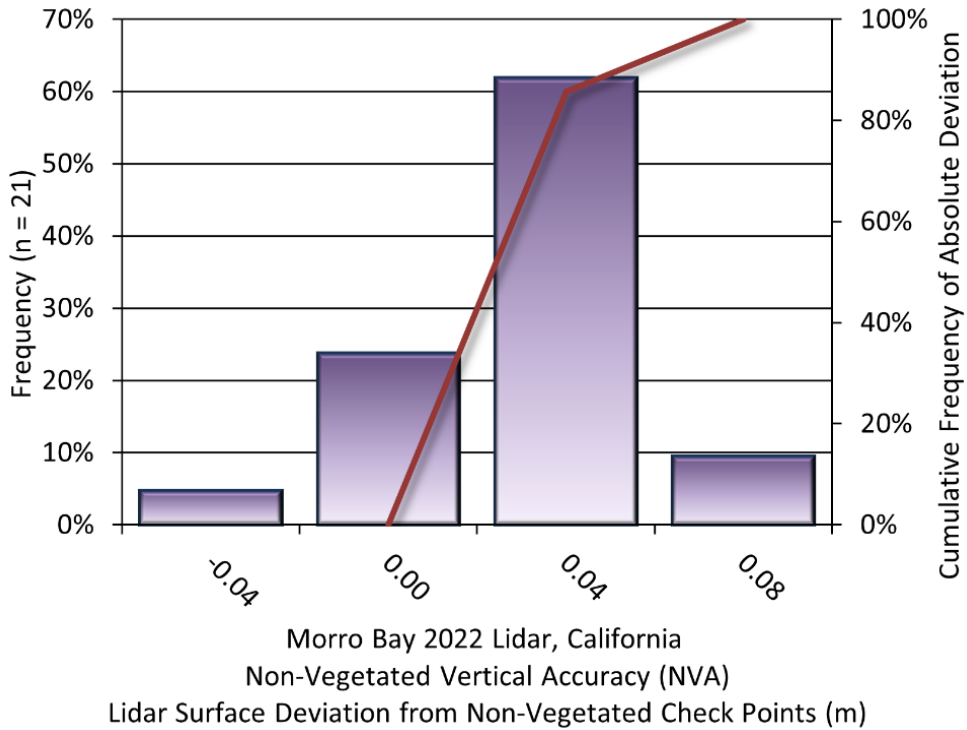


Figure 9: Frequency histogram for unclassified LAS deviation from ground check point values

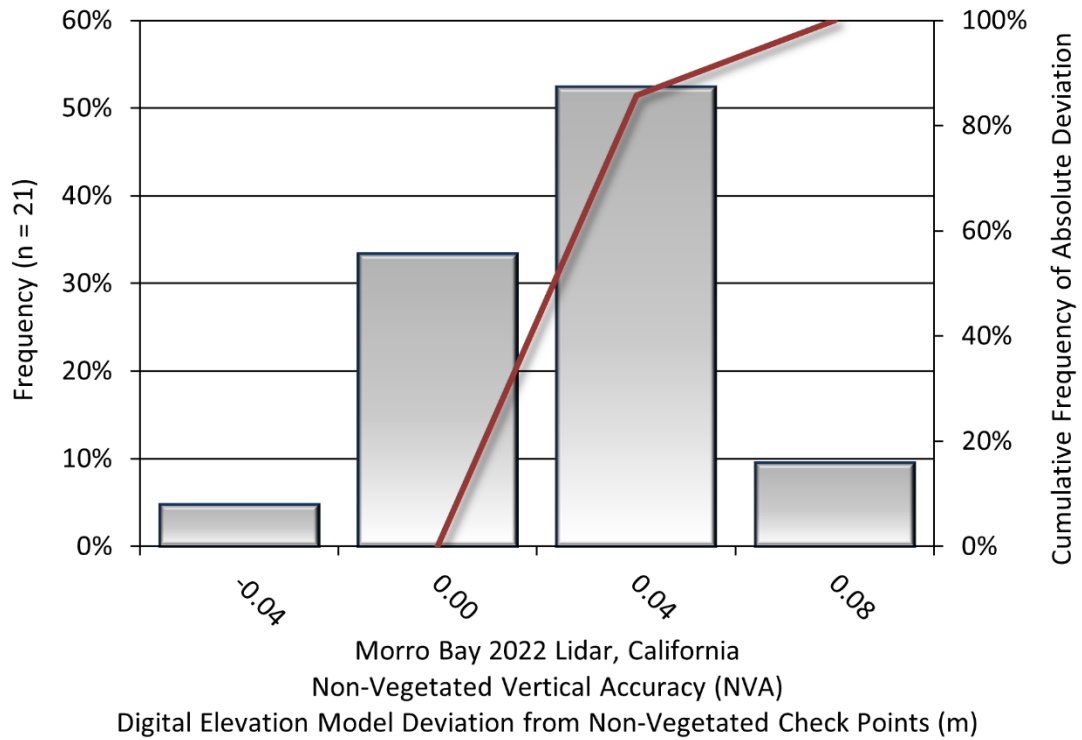


Figure 10: Frequency histogram for lidar bare earth DEM deviation from ground check point values

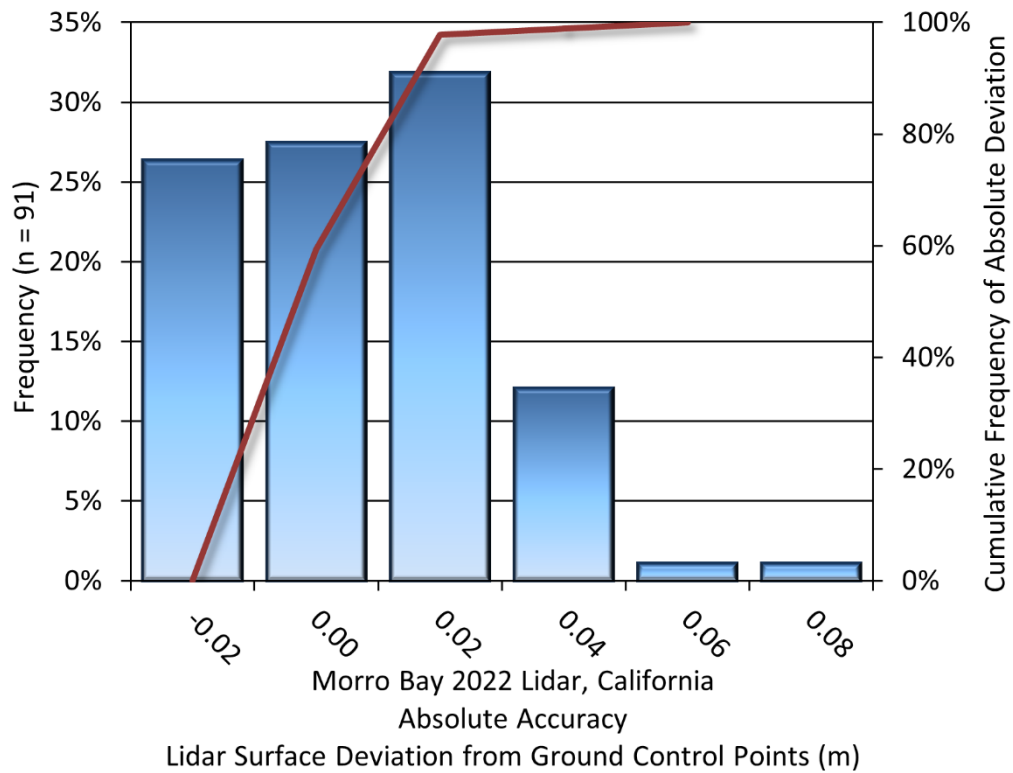


Figure 11: Frequency histogram for lidar surface deviation ground control point values

Lidar Bathymetric Vertical Accuracies

Bathymetric (submerged or along the water’s edge) check points were also collected in order to assess the submerged surface vertical accuracy. Assessment of 72 submerged bathymetric check points resulted in a vertical accuracy of 0.114 meters, while assessment of 30 wetted edge check points resulted in a vertical accuracy of 0.061 meters, evaluated at 95% confidence interval (Table 12, Figure 12, Figure 13).

Table 12: Bathymetric Vertical Accuracy for the Morro Bay Project

Parameter	Submerged Bathymetric Check Points	Wetted Edge Bathymetric Check Points
Sample	72 points	30 points
95% Confidence (1.96*RMSE)	0.114 m	0.061 m
Average Dz	0.036 m	0.009 m
Median	0.040 m	0.019 m
RMSE	0.058 m	0.031 m
Standard Deviation (1σ)	0.046 m	0.030 m

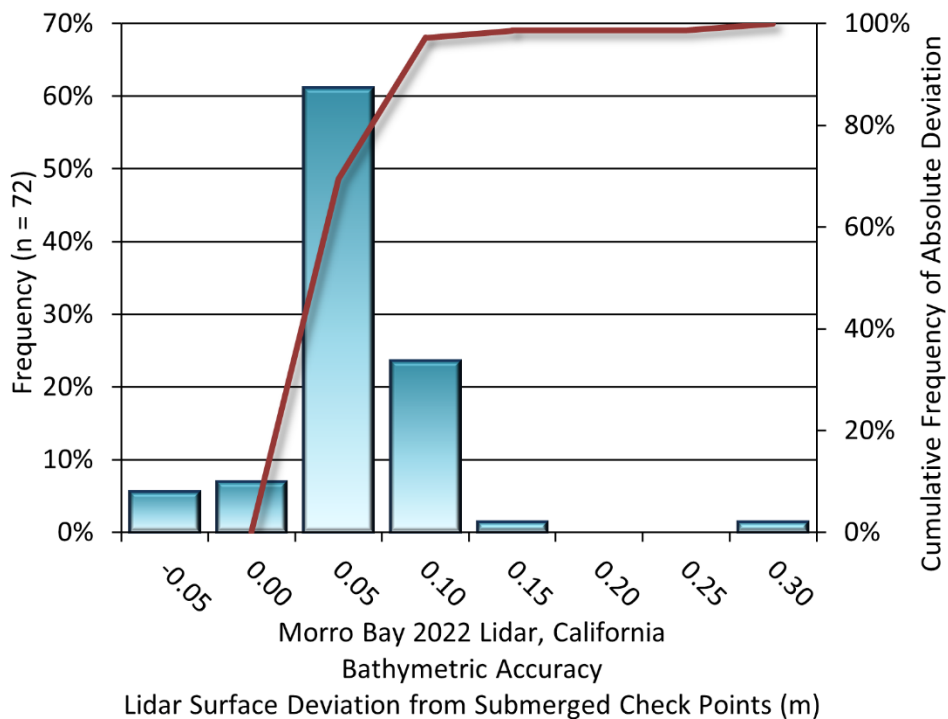


Figure 12: Frequency histogram for lidar surface deviation from submerged check point values

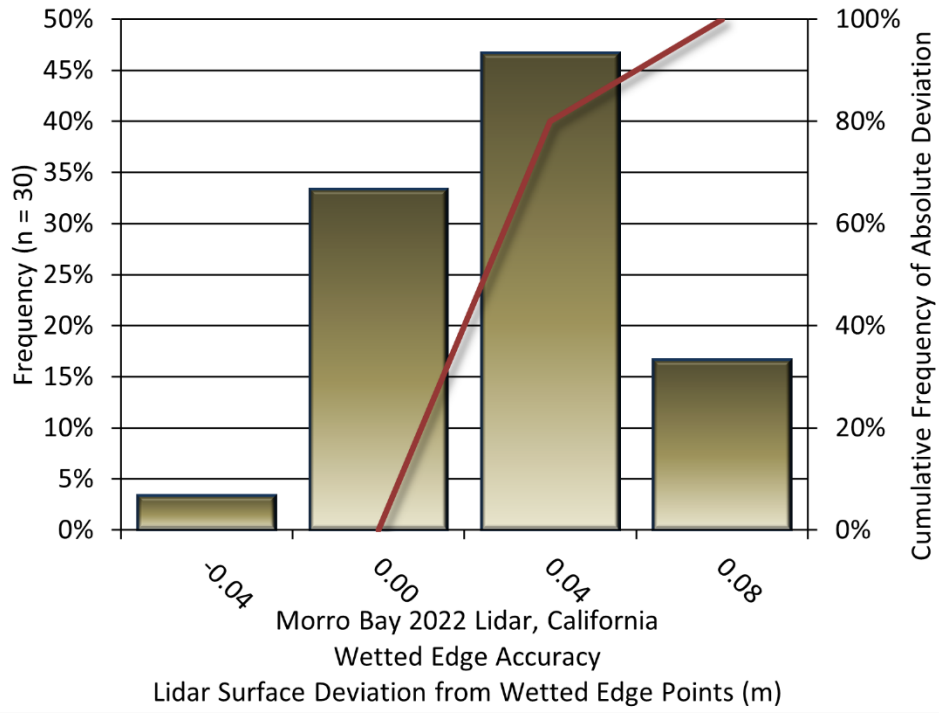


Figure 13: Frequency histogram for lidar surface deviation from wetted edge checkpoint values

Lidar Relative Vertical Accuracy

Relative vertical accuracy refers to the internal consistency of the data set as a whole: the ability to place an object in the same location given multiple flight lines, GPS conditions, and aircraft attitudes. When the lidar system is well calibrated, the swath-to-swath vertical divergence is low (<0.10 meters). The relative vertical accuracy was computed by comparing the ground surface model of each individual flight line with its neighbors in overlapping regions. The average (mean) line to line relative vertical accuracy for the Morro Bay lidar project was 0.018 meters (Table 13, Figure 14).

Table 13: Relative accuracy results

Parameter	Relative Vertical Accuracy
Sample	66 flight line surfaces
Average	0.018 m
Median	0.018 m
RMSE	0.023 m
Standard Deviation (1 σ)	0.010 m
1.96 σ	0.020 m

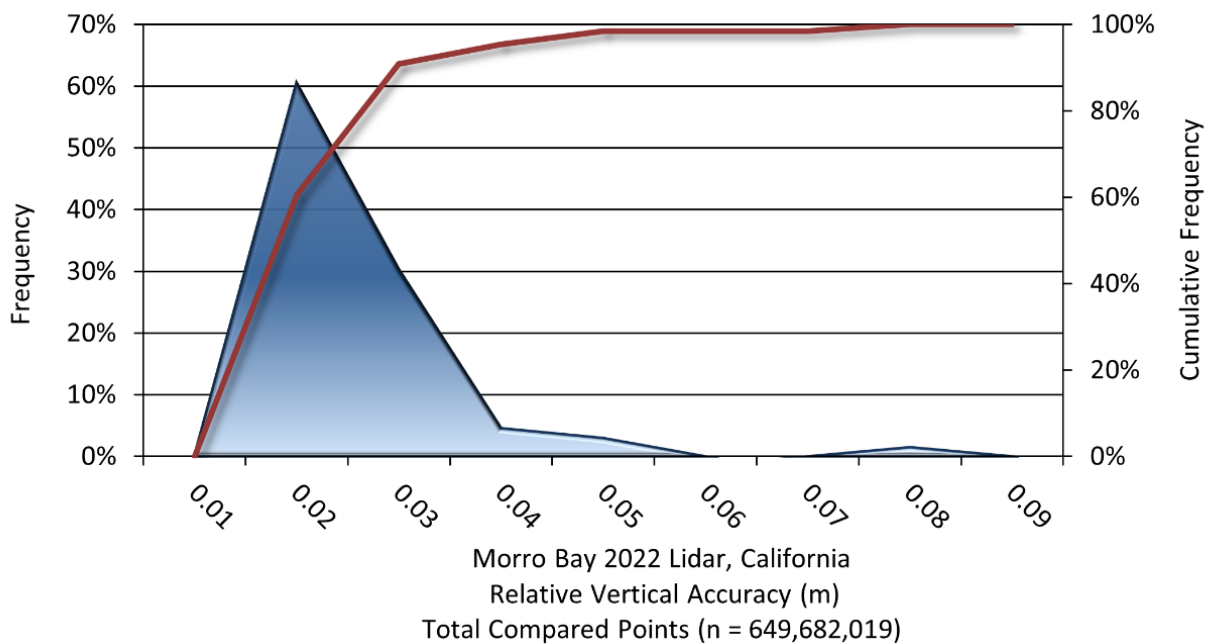


Figure 14: Frequency plot for relative vertical accuracy between flight lines

Lidar Horizontal Accuracy

Lidar horizontal accuracy is a function of Global Navigation Satellite System (GNSS) derived positional error, flying altitude, and INS derived attitude error. The obtained $RMSE_r$ value is multiplied by a conversion factor of 1.7308 to yield the horizontal component of the National Standards for Spatial Data Accuracy (NSSDA) reporting standard where a theoretical point will fall within the obtained radius 95 percent of the time. Based on a flying altitude of 400 meters, an IMU error of 0.002 decimal degrees, and a GNSS positional error of 0.023 meters, this project was compiled to meet 0.06 m horizontal accuracy at the 95% confidence level (Table 14).


Table 14: Horizontal Accuracy

Parameter	Horizontal Accuracy
$RMSE_r$	0.03 m
ACC_r	0.06 m

CERTIFICATIONS

NV5 Geospatial provided lidar services for the Morro Bay project as described in this report.

I, John English, have reviewed the attached report for completeness and hereby state that it is a complete and accurate report of this project.


John English (Oct 5, 2022 10:00 PDT)

Oct 5, 2022

John English
Project Manager
NV5 Geospatial

I, Evon P. Silvia, PLS, being duly registered as a Professional Land Surveyor in and by the state of California, hereby certify that the methodologies, static GNSS occupations used during airborne flights, and ground survey point collection were performed using commonly accepted Standard Practices. Field work conducted for this report was on 6/14/2022 and 6/15/2022.

Accuracy statistics shown in the Accuracy Section of this Report have been reviewed by me and found to meet the "National Standard for Spatial Data Accuracy".



Evon P. Silvia, PLS
NV5 Geospatial
Corvallis, OR 97330



Date Signed: Oct 5, 2022

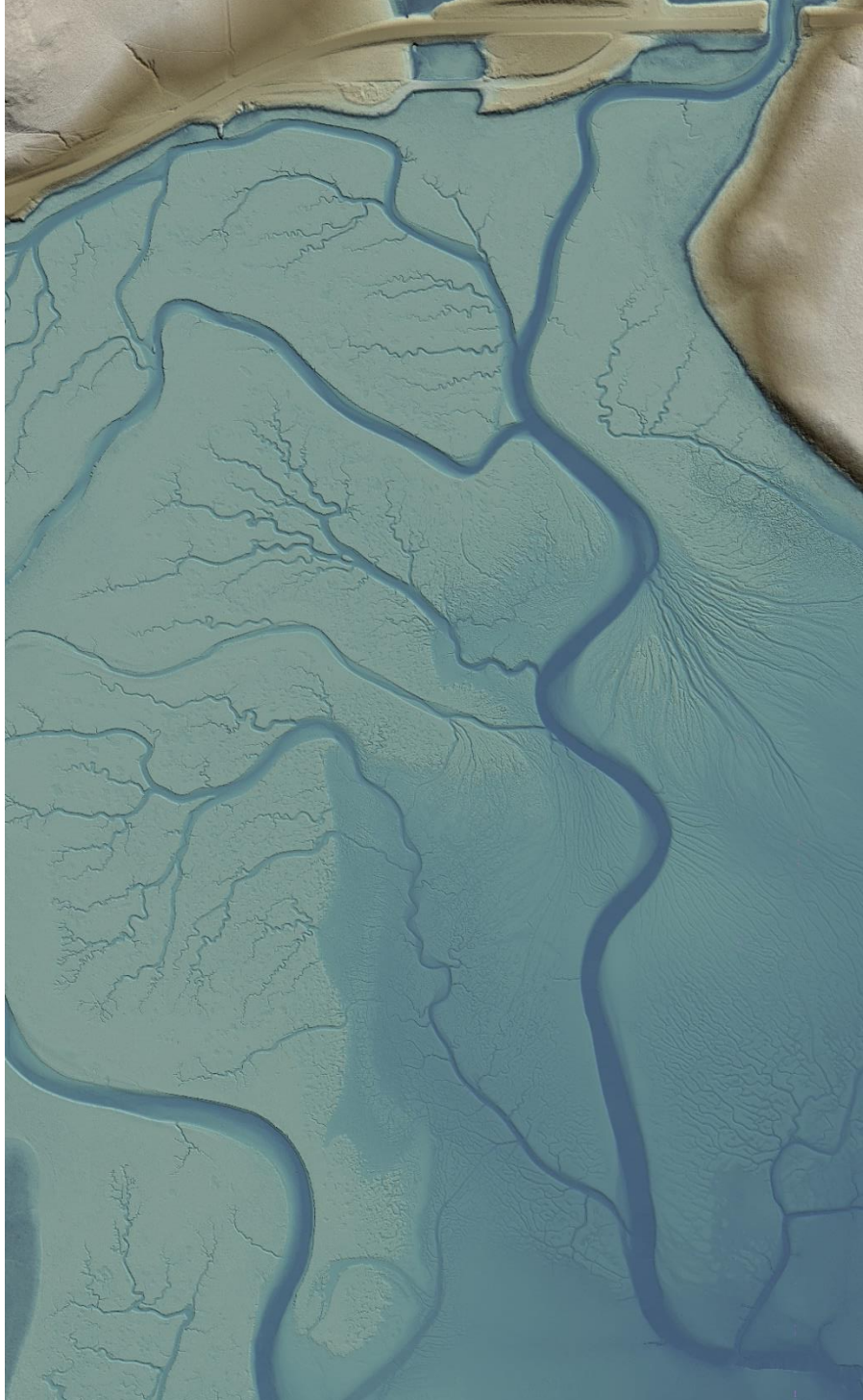


Figure 15: A top down view of the Morro Bay area of interest. This image was created from the lidar bare earth elevation model colored by elevation.

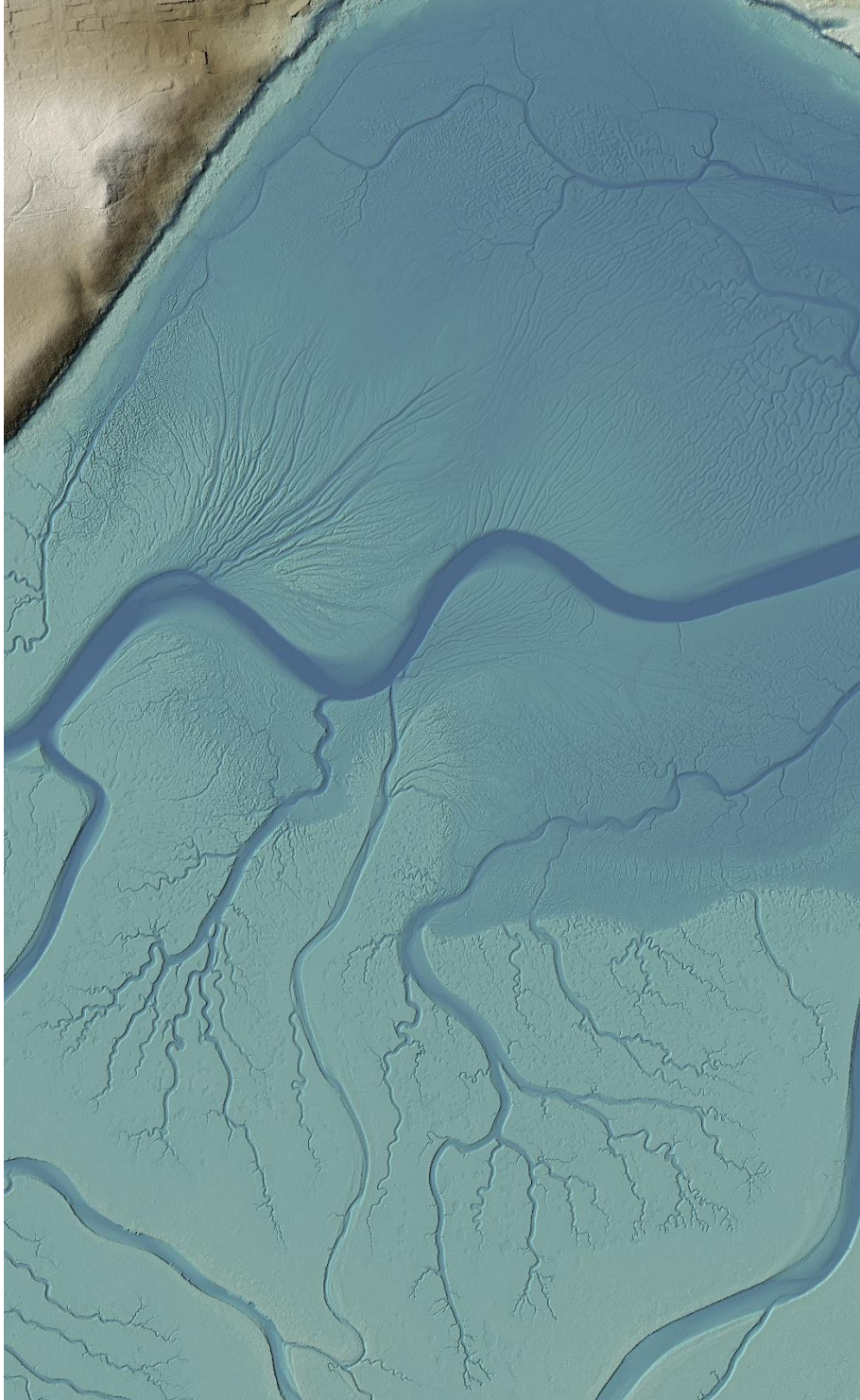


Figure 16: A top down view of the Morro Bay area of interest. This image was created from the lidar bare earth elevation model colored by elevation.

1-sigma (σ) Absolute Deviation: Value for which the data are within one standard deviation (approximately 68th percentile) of a normally distributed data set.

1.96 * RMSE Absolute Deviation: Value for which the data are within two standard deviations (approximately 95th percentile) of a normally distributed data set, based on the FGDC standards for Non-vegetated Vertical Accuracy (FVA) reporting.

Accuracy: The statistical comparison between known (surveyed) points and laser points. Typically measured as the standard deviation (σ) and root mean square error (RMSE).

Absolute Accuracy: The vertical accuracy of lidar data is described as the mean and standard deviation (σ) of divergence of lidar point coordinates from ground survey point coordinates. To provide a sense of the model predictive power of the dataset, the root mean square error (RMSE) for vertical accuracy is also provided. These statistics assume the error distributions for x, y and z are normally distributed, and thus we also consider the skew and kurtosis of distributions when evaluating error statistics.

Relative Accuracy: Relative accuracy refers to the internal consistency of the data set; i.e., the ability to place a laser point in the same location over multiple flight lines, GPS conditions and aircraft attitudes. Affected by system attitude offsets, scale and GPS/IMU drift, internal consistency is measured as the divergence between points from different flight lines within an overlapping area. Divergence is most apparent when flight lines are opposing. When the lidar system is well calibrated, the line-to-line divergence is low (<10 cm).

Root Mean Square Error (RMSE): A statistic used to approximate the difference between real-world points and the lidar points. It is calculated by squaring all the values, then taking the average of the squares and taking the square root of the average.

Data Density: A common measure of lidar resolution, measured as points per square meter.

Digital Elevation Model (DEM): File or database made from surveyed points, containing elevation points over a contiguous area. Digital terrain models (DTM) and digital surface models (DSM) are types of DEMs. DTMs consist solely of the bare earth surface (ground points), while DSMs include information about all surfaces, including vegetation and man-made structures.

Intensity Values: The peak power ratio of the laser return to the emitted laser, calculated as a function of surface reflectivity.

Nadir: A single point or locus of points on the surface of the earth directly below a sensor as it progresses along its flight line.

Overlap: The area shared between flight lines, typically measured in percent. 100% overlap is essential to ensure complete coverage and reduce laser shadows.

Pulse Rate (PR): The rate at which laser pulses are emitted from the sensor; typically measured in thousands of pulses per second (kHz).

Pulse Returns: For every laser pulse emitted, the number of wave forms (i.e., echoes) reflected back to the sensor. Portions of the wave form that return first are the highest element in multi-tiered surfaces such as vegetation. Portions of the wave form that return last are the lowest element in multi-tiered surfaces.

Real-Time Kinematic (RTK) Survey: A type of surveying conducted with a GPS base station deployed over a known monument with a radio connection to a GPS rover. Both the base station and rover receive differential GPS data and the baseline correction is solved between the two. This type of ground survey is accurate to 1.5 cm or less.

Post-Processed Kinematic (PPK) Survey: GPS surveying is conducted with a GPS rover collecting concurrently with a GPS base station set up over a known monument. Differential corrections and precisions for the GNSS baselines are computed and applied after the fact during processing. This type of ground survey is accurate to 1.5 cm or less.

Scan Angle: The angle from nadir to the edge of the scan, measured in degrees. Laser point accuracy typically decreases as scan angles increase.

Native Lidar Density: The number of pulses emitted by the lidar system, commonly expressed as pulses per square meter.

APPENDIX A - ACCURACY CONTROLS

Relative Accuracy Calibration Methodology:

Manual System Calibration: Calibration procedures for each mission require solving geometric relationships that relate measured swath-to-swath deviations to misalignments of system attitude parameters. Corrected scale, pitch, roll and heading offsets were calculated and applied to resolve misalignments. The raw divergence between lines was computed after the manual calibration was completed and reported for each survey area.

Automated Attitude Calibration: All data were tested and calibrated using TerraMatch automated sampling routines. Ground points were classified for each individual flight line and used for line-to-line testing. System misalignment offsets (pitch, roll and heading) and scale were solved for each individual mission and applied to respective mission datasets. The data from each mission were then blended when imported together to form the entire area of interest.

Automated Z Calibration: Ground points per line were used to calculate the vertical divergence between lines caused by vertical GPS drift. Automated Z calibration was the final step employed for relative accuracy calibration.

Lidar accuracy error sources and solutions:

Source	Type	Post Processing Solution
Long Base Lines	GPS	None
Poor Satellite Constellation	GPS	None
Poor Antenna Visibility	GPS	Reduce Visibility Mask
Poor System Calibration	System	Recalibrate IMU and sensor offsets/settings
Inaccurate System	System	None
Poor Laser Timing	Laser Noise	None
Poor Laser Reception	Laser Noise	None
Poor Laser Power	Laser Noise	None
Irregular Laser Shape	Laser Noise	None

Operational measures taken to improve relative accuracy:

Focus Laser Power at narrow beam footprint: A laser return must be received by the system above a power threshold to accurately record a measurement. The strength of the laser return (i.e., intensity) is a function of laser emission power, laser footprint, flight altitude and the reflectivity of the target. While surface reflectivity cannot be controlled, laser power can be increased and low flight altitudes can be maintained.

Reduced Scan Angle: Edge-of-scan data can become inaccurate. The scan angle was reduced to a maximum of $\pm 20^\circ$ to $\pm 21^\circ$ from nadir, creating a narrow swath width and greatly reducing laser shadows from trees and buildings.

Quality GPS: Flights took place during optimal GPS conditions (e.g., 6 or more satellites and PDOP [Position Dilution of Precision] less than 3.0). Before each flight, the PDOP was determined for the survey day. During all flight times, a dual frequency DGPS base station recording at 1 second epochs was utilized and a maximum baseline length between the aircraft and the control points was less than 13 nm at all times.

Ground Survey: Ground survey point accuracy (<1.5 cm RMSE) occurs during optimal PDOP ranges and targets a minimal baseline distance of 4 miles between GPS rover and base. Robust statistics are, in part, a function of sample size (n) and distribution. Ground survey points are distributed to the extent possible throughout multiple flight lines and across the survey area.

50% Side-Lap (100% Overlap): Overlapping areas are optimized for relative accuracy testing. Laser shadowing is minimized to help increase target acquisition from multiple scan angles. Ideally, with a 50% side-lap, the nadir portion of one flight line coincides with the swath edge portion of overlapping flight lines. A minimum of 50% side-lap with terrain-followed acquisition prevents data gaps.

Opposing Flight Lines: All overlapping flight lines have opposing directions. Pitch, roll and heading errors are amplified by a factor of two relative to the adjacent flight line(s), making misalignments easier to detect and resolve.